

# **CP VIOLATION IN ATOMIC AND NUCLEAR PHYSICS**

E. D. Commins

Physics Dept., University of California

and

E. O. Lawrence Berkeley National Laboratory

Berkeley, California 94720

## **ABSTRACT**

CP violation and CPT invariance imply T- violation, which should appear at some level in atomic and nuclear phenomena. In this report we briefly summarize various experiments to search for T-violating strong interactions and weak decays, and discuss in some detail various searches for electric dipole moments of elementary particles, nuclei, atoms, and molecules.

# 1 Introduction

CP violation and CPT invariance imply T-violation, which is expected to occur at some level in atomic and nuclear phenomena. For example if both P and T are violated, an elementary particle, nucleus, atom, or molecule can possess a permanent electric dipole moment (EDM). This happens because CP violation and the usual weak interaction must induce EDM's at some level by means of radiative corrections to the P,C,T conserving electromagnetic interaction. Searches for EDM's began 50 years ago, 6 years before the discovery of P-violation in the weak interactions, 7 years before it was realized that EDM's violate T-invariance, and 14 years before the discovery of CP-violation in kaon decay. EDM searches, which have so far yielded only upper limits, continue unabated today. In the aftermath of the discovery of parity violation in 1956-57, several other types of experiments to search for T-violation were launched: "direct" searches for T-violation in strong interactions, "triple correlations" in nuclear beta decay, etc. These have also yielded only upper limits so far. Thus one may say that progress in our field is glacial, at best. In this report we devote most of our attention to electric dipole moments, since in the general view this is the area where positive results are most likely to emerge. But we first summarize very briefly the direct tests of T-invariance in strong interactions, and the triple correlation measurements in nuclear beta decay.

Before we begin our survey, however, let's recall what time reversal invariance means. The (anti-unitary) time reversal operation reverses all momenta and spins, and interchanges initial and final states. Consider one or more particles in an initial state A with linear momenta  $\mathbf{p}_i$  and spins  $s_i$ . Suppose this system undergoes a transition (by decay or collision) to a final state B consisting of particles with linear momenta  $\mathbf{p}_f, \mathbf{s}_f$ . We can describe the transition by an S-matrix element:

$$S_{BA} = \delta_{BA} - iK_{BA} \quad (1)$$

where K is the transition operator:

$$K_{BA} = \langle B(\mathbf{p}_f, \mathbf{s}_f) | K | A(\mathbf{p}_i, \mathbf{s}_i) \rangle \quad (2)$$

Thus the time-reversed transition matrix element is:

$$K'_{AB} = \langle A(-\mathbf{p}_i, -\mathbf{s}_i) | K | B(-\mathbf{p}_f, -\mathbf{s}_f) \rangle \quad (3)$$

By definition, time reversal invariance holds for the reaction if

$$|K'_{AB}| = |K_{BA}| \quad (4)$$

## 2 Direct tests of T-invariance in the Strong Interaction

Experimental tests of the discrete symmetries P, C, and T in the strong interaction have very limited precision. From numerous studies of parity violation in nuclear forces (a phenomenon that is attributed to the charged- and neutral-weak interactions of nucleons), we can say that P is conserved in strong interactions to about 10 ppm.<sup>1</sup> Comparison of the rates of certain strong reactions such as  $p\bar{p} \rightarrow \bar{K}^0 K^+ \pi^-$  and  $p\bar{p} \rightarrow K^0 K^- \pi^+$  tells us that the strong interaction is C-conserving to about 1% precision.<sup>2</sup> As for time reversal, the most direct experimental tests involve measurement of the differential cross sections for a certain nuclear reaction and its inverse<sup>3</sup>:



studies of the statistics of compound nucleus energy level distributions,<sup>4</sup> and observation of the transmission of low-energy polarized neutrons through a target of aligned  ${}^{165}\text{Ho}$  nuclei.<sup>5</sup> In the latter case one searches for the correlation  $\boldsymbol{\sigma} \cdot (\mathbf{k} \times \mathbf{I})\mathbf{k} \cdot \mathbf{I}$  where  $\boldsymbol{\sigma}$ ,  $\mathbf{k}$ , and  $\mathbf{I}$  refer to the neutron spin, neutron momentum, and nuclear spin respectively. In all of these cases one is looking for a T-violating, P-conserving (TVPC) effect. The result of these experiments is expressed in terms of the ratio  $\alpha_T$  of the TVPC transition matrix element to the usual T, P conserving strong interaction matrix element. One is able to obtain only a very crude limit:  $\alpha_T \lesssim 3 \cdot 10^{-3}$ , which corresponds to a mass scale  $\Lambda_T \gtrsim 10$  GeV for new TVPC physics beyond the standard model. Clearly, 10 GeV is a very low mass scale, and intuitively it would seem to be very unlikely.

Recently Ramsey-Musolf<sup>6</sup> has shown that a far more stringent limit:  $\Lambda_{\text{TVPC}} \gtrsim 150$  TeV, corresponding to  $\alpha_T \lesssim 10^{-15}$ , can be obtained indirectly by combining the upper limits obtained from neutron and electron electric dipole moment experiments (to be discussed below) with an analysis of radiative corrections based on the standard model. The basic idea is that P, C violating standard model weak interactions at the radiative correction level would necessarily combine with C, T violating strong interactions, if they were to exist, to produce P, T violating EDM's.

## 3 Triple correlations in weak decays

How can we test for T-violation in weak decays? Let us consider neutron beta decay as a typical example:  $n \rightarrow pe^- \bar{\nu}_e$ . Obviously it is impossible to check time reversal invariance by running this reaction backward! However, there is a useful indirect alternative.

Consider once again the S operator:

$$S = I - iK \quad (6)$$

Since S is unitary, we have:

$$\begin{aligned} I &= SS^\dagger \\ &= (I - iK)(I + iK^\dagger) \\ &= I - iK + iK^\dagger + KK^\dagger \end{aligned}$$

If K is sufficiently small, we can neglect  $KK^\dagger$ , in which case  $K = K^\dagger$ . Then,

$$K_{BA} = \langle B(\mathbf{p}_f, \mathbf{s}_f) | K | A(\mathbf{p}_i, \mathbf{s}_i) \rangle = \langle A(\mathbf{p}_i, \mathbf{s}_i) | K | B(\mathbf{p}_f, \mathbf{s}_f) \rangle^* \quad (7)$$

Meanwhile from (3) the time reversed transition amplitude is given by:

$$K'_{AB} = \langle A(-\mathbf{p}_i, -\mathbf{s}_i) | K | B(-\mathbf{p}_f, -\mathbf{s}_f) \rangle \quad (8)$$

Therefore, we have time reversal invariance if:

$$|\langle B(-\mathbf{p}_f, -\mathbf{s}_f) | K | A(-\mathbf{p}_i, -\mathbf{s}_i) \rangle| = |\langle B(\mathbf{p}_f, \mathbf{s}_f) | K | A(\mathbf{p}_i, \mathbf{s}_i) \rangle| \quad (9)$$

provided, always, that we can assume  $K = K^\dagger$ . Of course for the weak interaction itself this is a good assumption, but the matrix element refers to initial and final *physical states*, and we must remember that the final states are always affected to some extent by *final state interaction*. Thus result (9) is valid only to the extent to which we can neglect final state corrections.

With this in mind, let us consider neutron decay as viewed in the neutron rest frame. Fig.1a shows a neutron with spin up (out of the page) decaying to a proton, electron, and anti-neutrino (with linear momenta in the plane of the page). For simplicity we shall ignore the spins of the final particles. Suppose the amplitude corresponding to Fig.1a is  $M$ . In Fig. 1b, the momenta and spins are the same, but initial and final states are reversed. The corresponding amplitude is  $M^*$ . Now in Fig. 1c we perform the time reversal operation on the system of Fig. 1b. This means that momenta and spins are reversed, and initial and final states are once more interchanged. The corresponding amplitude is  $M^{*l}$ . Notice that apart from a 180 deg rotation about the neutron spin axis, the final particle momenta are the same as in Fig. 1a, but the neutron spin is reversed. If time reversal invariance holds, the probabilities for Figs. 1a and 1c should be the same;

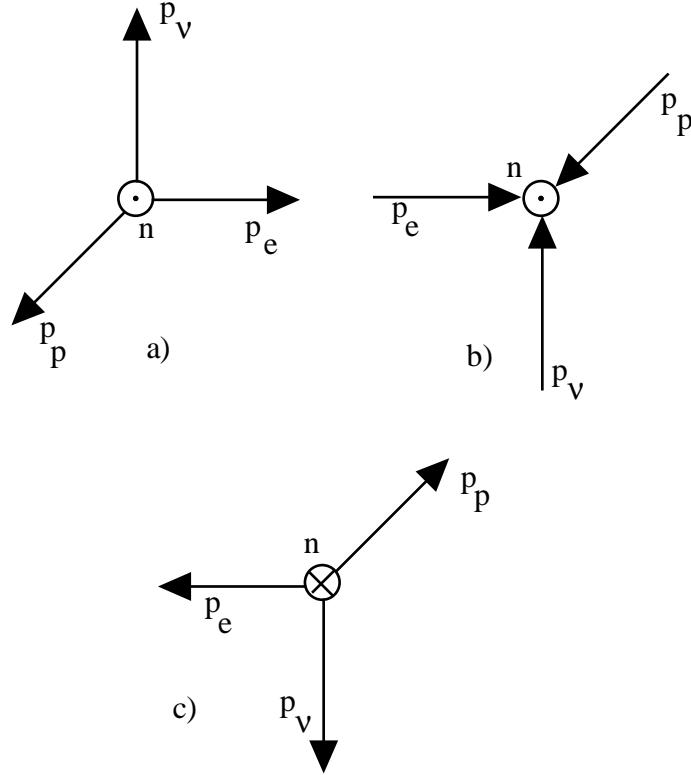


Fig. 1. a) A neutron with spin up (out of page) decays to proton,  $e^-$ , and  $\bar{\nu}$  with momenta in plane of page. Amplitude= $M$ . b) Initial and final states interchanged; amplitude= $M^*$ . c) Process of 1b time-reversed: Amplitude  $M^{*'}$ .

in other words, there should be no observable correlation of the form:  $\sigma_n \cdot \mathbf{p}_e \times \mathbf{p}_\nu$ . Now let's consider the same thing in more detail. Years ago, Jackson, Treiman, and Wyld<sup>7</sup> showed that, neglecting nuclear recoil and final state interactions, the differential transition probability per unit time for beta decay of polarized nuclei with spin 1/2 in the allowed approximation, summed over final spins, is given by:

$$\begin{aligned}
 dW &= \frac{G_F^2}{(2\pi)^5} \cos^2 \theta_C \delta(E_e + E_\nu - \Delta) \\
 &\times F(Z, E_e) d^3 \mathbf{p}_e d^3 \mathbf{p}_\nu \\
 &\times \xi \left[ 1 + a \frac{\mathbf{p}_e \cdot \mathbf{p}_\nu}{E_e E_\nu} + \frac{\langle \mathbf{J}_i \rangle}{J_i} \left( A \frac{\mathbf{p}_e}{E_e} + B \frac{\mathbf{p}_\nu}{E_\nu} + D \frac{\mathbf{p}_e \times \mathbf{p}_\nu}{E_e E_\nu} \right) \right] \quad (10)
 \end{aligned}$$

where  $\hbar = c = 1$ ,  $G_F$  is Fermi's constant,  $\theta_C$  is the Cabibbo angle,  $\Delta$  is the maximum electron energy,  $F(Z, E_e)$  is the Coulomb correction factor, and  $\mathbf{J}_i$  is the initial nuclear

spin. Also,

$$\xi = |C_V|^2 |\langle 1 \rangle|^2 + |C_A|^2 |\langle \sigma \rangle|^2 \quad (11)$$

and  $C_{V,A}$  are the vector and axial vector coupling constants, respectively;  $\langle 1 \rangle$  and  $\langle \sigma \rangle$  are the Fermi and Gamow-Teller reduced matrix elements, respectively;  $a$  is the neutrino-electron momentum correlation coefficient,  $A$  is the beta asymmetry parameter,  $B$  is the analogous parameter for the neutrino, and:

$$\xi D = i(C_V C_A^* - C_A C_V^*) \langle 1 \rangle \langle \sigma \rangle \left( \frac{J_i}{J_i + 1} \right)^{1/2} \quad (12)$$

It is the "triple correlation" coefficient  $D$  that is of interest here. In the approximation where we neglect final state interaction,  $D$  can only be non-zero if there is T-violation since T-invariance requires that  $C_V$  and  $C_A$  be relatively real.

The  $D$  coefficient has been studied experimentally in neutron decay and in the super-allowed beta decay  $^{19}\text{Ne} \rightarrow ^{19}\text{F} + e^+ + \nu_e$ . The only significant final state correction to  $D$  in each of these decays arises from interference between the Coulomb interaction of the final nucleus and emitted electron, and the "weak magnetism" portion of the weak vector amplitude.<sup>8</sup> It can be shown that:

$$\begin{aligned} D_n^{WM} &= \frac{E_e^2}{p_e m_n} (-0.032 + 0.040 \frac{m_e^2}{E_e}) \\ &= -5.7 \cdot 10^{-5} \text{ at } \textit{max } p_e \end{aligned} \quad (13)$$

and

$$D_{neon}^{WM} \approx 3 \cdot 10^{-4} \quad (14)$$

The present experimental limits on  $D$  are summarized in Table 1. The recent N.I.S.T. neutron experiment was designed to yield a substantial improvement in precision compared to the older I.L.L. and Kurtchatov results, but due to various experimental difficulties, the results have so far been disappointing. Theoretical limits on  $D$  (see Table 2) are very-model dependent. According to the standard model, and to a number of currently popular models for physics beyond the standard model,  $D$  is far too small to be observed in any practical experiment, now or in the foreseeable future. The only existing models that can yield predictions for  $D$  close to present experimental limits are those that invoke the existence of leptoquarks.

We have just considered experiments in nuclear beta decay where one sums over all final spins. However, if one can detect the spin of the final electron or positron, the following T-odd terms in the transition probability are observable:

$$R\boldsymbol{\sigma}_n \cdot (\boldsymbol{\sigma}_e \times \mathbf{p}_e)$$

$$L\boldsymbol{\sigma}_e \cdot (\mathbf{p}_e \times \mathbf{p}_\nu).$$

The correlation coefficient L has never been measured in any decay. R has been observed in  ${}^8\text{Li}$  decay:

$$R({}^8\text{Li}) = (0.9 \pm 2.2) \cdot 10^{-3} \quad (15)$$

and a measurement in neutron decay has been discussed. However,  $R=0$  for pure V, A interaction regardless of the relative phase of V and A amplitudes. Non-zero R requires interference between scalar and axial vector, and/or interference between tensor and vector couplings. Khriplovich<sup>9</sup> has shown that indirect limits on T-odd scalar and tensor couplings in beta decay obtained from neutron and electron EDM results, together with calculated standard model radiative corrections, are far more sensitive than the limits that can be obtained from direct measurements in beta decay.

Table 1. Measurements of D

Initial nucleus	D	Ref.
neutron	$(-1.1 \pm 1.7) \cdot 10^{-3}$ (I.L.L.)	10
neutron	$(2.2 \pm 3.0) \cdot 10^{-3}$ (Kurtchatov)	11
neutron	$(-0.1 \pm 1.3 \pm 0.7) \cdot 10^{-3}$ (N.I.S.T.)	12
${}^{19}\text{Ne}$	$(4 \pm 8) \cdot 10^{-4}$ (Princeton)	13

Table 2. Theoretical limits on D

Theoretical model	D
Standard model	$< 10^{-12}$
Theta-QCD	$< 10^{-12}$
Supersymmetry	$< 10^{-6}$
Left-right symmetry	$< 10^{-4}$
Exotic fermion	$< 10^{-4}$
Leptoquark models	Limited by expt.

Finally, consider the decay  $K^+ \rightarrow \pi^0 \mu^+ \nu_\mu$ . The "transverse muon polarization"  $P_T$  in this decay is the component of muon polarization perpendicular to the plane of the final momenta. Observation of  $P_T$ , that is, observation of a triple correlation of the form  $\boldsymbol{\sigma}_\mu \cdot \mathbf{p}_\pi \times \mathbf{p}_\mu$ , would constitute evidence for T-violation, since at the level of precision

attainable with present methods, final-state corrections are negligible. According to the standard model,  $P_T$  should be  $\approx 10^{-7}$ . Very recently, the following experimental result was obtained<sup>14</sup>:

$$P_T = -0.0042 \pm 0.0049(stat) \pm 0.0009(syst) \quad (16)$$

## 4 General remarks about electric dipole moments

We have already mentioned that an elementary particle, nucleus, atom, or molecule can only possess an electric dipole moment (EDM) if both P and T are violated. This can be seen<sup>15</sup> in a very simple way as follows. Consider a particle of spin 1/2 and assume that it has an EDM  $\mathbf{d}$  as well as a spin magnetic dipole moment  $\boldsymbol{\mu}$ . Both moments lie along the spin direction, because the spin is the only vector available to orient the particle. We write the Hamiltonians  $H_M, H_E$  that describe the interaction of  $\boldsymbol{\mu}$  with a magnetic field  $\mathbf{B}$ , and of  $\mathbf{d}$  with an electric field  $\mathbf{E}$ , in the non-relativistic limit:

$$H_M = -\boldsymbol{\mu} \cdot \mathbf{B} = -\mu \boldsymbol{\sigma} \cdot \mathbf{B} \quad (17)$$

$$H_E = -\mathbf{d} \cdot \mathbf{E} = -d \boldsymbol{\sigma} \cdot \mathbf{E} \quad (18)$$

where  $\boldsymbol{\sigma}$  is the Pauli spin operator. Under space inversion (P) the axial vectors  $\boldsymbol{\sigma}$  and  $\mathbf{B}$  remain unchanged, but the polar vector  $\mathbf{E}$  changes sign. Hence under P,  $H_M$  is invariant, while  $H_E$  is not. Under time reversal,  $\boldsymbol{\sigma}$  and  $\mathbf{B}$  change sign, while  $\mathbf{E}$  remains unchanged. Hence under T,  $H_M$  is once again invariant, but  $H_E$  changes sign.

Note that the P,T-violating EDMs of interest to us are not at all the same as the so-called "permanent" electric dipole moments of polar molecules, so well known to chemists and molecular spectroscopists. The latter are not really permanent at all and involve no violation of P or T. A very clear quantum-mechanical description of their behavior was already given in 1931 by Penney.<sup>16</sup>

It is impossible to form an intuitive classical picture of the EDM of an elementary particle (e.g. an electron); but it is just as impossible to make a classical model of the spin magnetic moment. Of course, the latter has become very familiar after 75 years, and we all have the illusion that we understand it thoroughly. We know that the Dirac equation for the electron contains the implication that the electron possesses a "normal" spin magnetic moment with the g-value:  $g_S = 2$ . We also know that a spin 1/2 particle with an anomalous magnetic moment can still be described by a Dirac-like

equation provided we add a gauge-invariant, Lorentz-invariant Pauli moment term. In field theory this is described by the well-known Lagrangian density:

$$\mathcal{L}_{Pauli} = -\kappa \frac{\mu_B}{2} \bar{\Psi} \sigma^{\mu\nu} \Psi F_{\mu\nu} \quad (19)$$

Here  $\Psi$  is the Dirac field for the fermion in question,  $\bar{\Psi}$  is the Dirac conjugate field,  $\sigma^{\mu\nu} = \frac{i}{2}(\gamma^\mu \gamma^\nu - \gamma^\nu \gamma^\mu)$  where  $\gamma^\mu, \gamma^\nu$  are the usual 4x4 matrices,  $F_{\mu\nu}$  is the electromagnetic field tensor,  $\mu_B$  is the Bohr magneton, and  $\kappa$  is an appropriate constant. This Lagrangian density is of course invariant under P and T. To describe an EDM  $d$  we construct an analogous P-odd, T-odd Lagrangian density by making the replacements:  $\sigma^{\mu\nu} \rightarrow \gamma^5 \sigma^{\mu\nu}$  and  $\kappa \mu_B \rightarrow id$  where  $i = (-1)^{1/2}$  is necessary so that the resulting Hamiltonian shall be Hermitian. Thus<sup>17</sup> we obtain:

$$\mathcal{L}_{EDM} = -i \frac{d}{2} \bar{\Psi} \gamma^5 \sigma^{\mu\nu} \Psi F_{\mu\nu} \quad (20)$$

From this Lagrangian density, one can easily obtain the following single-particle EDM Hamiltonian:

$$H_{EDM} = -d \gamma^0 \boldsymbol{\Sigma} \cdot \mathbf{E} + id \boldsymbol{\gamma} \cdot \mathbf{B} \quad (21)$$

where

$$\boldsymbol{\Sigma} = \begin{pmatrix} \boldsymbol{\sigma} & 0 \\ 0 & \boldsymbol{\sigma} \end{pmatrix}$$

In the non-relativistic limit the first term on the right hand side of (21) reduces to the right hand side of (18). However, in general the factor  $\gamma^0$  is extremely important, as we shall see. The second term on the right hand side of (21) gives no contribution in the non-relativistic limit.

The EDM Lagrangian density  $\mathcal{L}_{EDM}$  is not renormalizable, and yields an EDM only by virtue of loop corrections to the usual fermion-photon interaction of quantum electrodynamics. The possible loop corrections are naturally very model-dependent and uncertain. For, while the parameters that describe CP violation in kaon decay have been measured ever more precisely over the years, the fundamental explanation for CP violation remains very much in doubt, and a wide variety of plausible, if very speculative, models of CP violation have been presented. According to the standard model, the electron EDM  $d_e$ , the neutron EDM  $d_n$ , and other EDM's as well are far too small to be detected by any possible experiment, now or in the foreseeable future. However, in various extensions of the standard model (See Table 3)  $d_e$  and/or  $d_n$  are sufficiently large to be detected by practical experiments. In some models, even the

muon EDM  $d_\mu$  and/or the tau EDM  $d_\tau$  might be detectable, although less sensitive experimental methods are available for them than for  $d_e$  or  $d_n$ .

Table 3. Theoretical predictions for neutron, electron EDMs

CP Viol Model	Neutron (e cm)	Electron (e cm)
Standard	$10^{-32} - 10^{-34}$	$\approx 10^{-40}$
Minimal SUSY	$10^{-25} - 10^{-26}$	$10^{-26} - 10^{-28}$
SUSY GUT [SO(10)]	$10^{-25} - 10^{-27}$	$10^{-26} - 10^{-28}$
L-R Symmetric	$10^{-25} - 10^{-26}$	$10^{-26} - 10^{-28}$
Multi-Higgs	$10^{-25} - 10^{-26}$	$10^{-26} - 10^{-28}$
Lepton-flavor changing	—	$10^{-27} - 10^{-29}$

Why does the standard model predict that  $d_e$  and  $d_n$  are so small? In the standard model, the neutron EDM could arise from valence quark EDMs but this cannot occur at the one-loop level. At the two-loop level individual diagrams do have complex phases that contribute to  $d_n$  but it has been shown<sup>18</sup> that the sum of these diagrams over all quark flavors yields zero. Thus, according to the standard model, the neutron EDM appears only at the 3-loop level, and even here there are suppressions and cancellations.<sup>19</sup>

In the standard model with massless neutrinos there is no analog to the CKM matrix in the lepton sector, and thus no analogous way to generate CP violation. For the electron EDM to arise here we would require coupling to virtual quarks via virtual  $W^\pm$ . Naively one might expect a contribution from the two-loop diagram of Fig.2. However, for each contribution  $V_{ij}$  from the CKM matrix at one vertex, there is a contribution  $V_{ij}^*$  at the other vertex; hence the overall amplitude cannot contain a CP violating phase. (This is also the reason why there is no neutron EDM at the one-loop level).

Next, one can consider contributions to the electron EDM at the 3-loop level. This situation was first analyzed by Hoogeveen<sup>20</sup> but it was subsequently shown by Pospelov and Khriplovich<sup>21</sup> that the various 3-loop diagrams cancel, yielding a net contribution of zero in the absence of gluonic corrections to the quark lines (see Fig. 3).

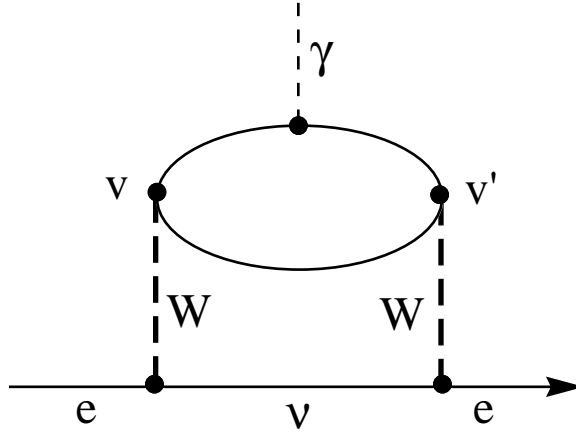


Fig. 2. This two-loop diagram cannot contribute to the electron EDM, because although a factor  $V_{ij}$  from the CKM matrix appears at vertex  $v$ , a factor  $V_{ij}^*$  appears at vertex  $v'$ . Thus, there is no net CP-violating phase.

## 5 The neutron EDM

In neutron EDM experiments one employs Ramsey's method<sup>22</sup> of separated oscillating magnetic fields to observe magnetic resonance on the neutron spin-magnetic moment in a fixed static magnetic field  $\mathbf{B}$ . An electric field  $\mathbf{E}$  parallel or anti-parallel to  $\mathbf{B}$  is inserted between the oscillating fields. The basic idea is that the interaction  $H_E = -\mathbf{d} \cdot \mathbf{E}$  might cause a detectable frequency shift in the magnetic resonance fringe pattern. In the earliest neutron EDM experiments this was done with neutron beams, and the oscillating fields were separated spatially. Modern neutron EDM experiments make use of ultra-cold (UC) neutrons (which typically have kinetic energies of  $10^{-7} eV$  or less.) Such experiments take advantage of the fact that UC neutrons undergo critical reflection at any angle of incidence on suitable materials, and can thus be stored in closed vessels. Here, neutron storage bottles with collinear  $\mathbf{E}$  and  $\mathbf{B}$  fields, and oscillating fields separated *temporally* rather than spatially, are employed. Fig. 4 shows the apparatus employed for the 1990 neutron EDM experiment at Institut Laue-Langevin (I.L.L.) in Grenoble.<sup>23</sup> Ultra-cold neutrons were transported from the source through a guide tube and polarized by transmission through a magnetically saturated  $1\mu$  thick iron-cobalt

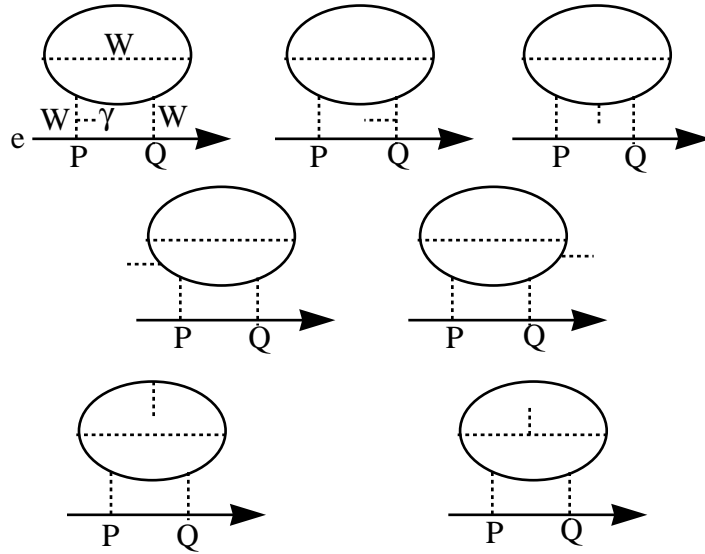


Fig. 3. The sum of the contributions to  $d_e$  from these 3-loop diagrams is zero, according to the standard model. If each diagram is disconnected from the lepton line at P,Q one has the 2-loop contributions to the EDM of an (on-mass-shell) W boson. Thus the EDM of a W boson is zero in the 2-loop approximation.

foil. The 5 liter storage bottle was enclosed by two beryllium electrodes 25 cm in diameter and a 10 cm long insulating cylinder of BeO. The static magnetic field was .01 Gauss in magnitude, and the electrodes were used to generate an electric field of 16000 V/cm. Neutrons could be admitted to the bottle by means of a beryllium valve in the grounded electrode. The experiment functioned as follows: the interaction volume was filled with UC polarized neutrons for 10 s. (3 filling time constants) and the beryllium valve was then closed. At this point the neutron number density was approximately  $10 \text{ cm}^{-3}$ . After a 6s. delay to allow the neutron velocities to be randomized, a first Ramsey pulse was applied for 4s., the neutrons were allowed to precess for 70s. in E and B fields, and then a second 4s. Ramsey pulse was applied. Subsequently the valve was opened, neutrons in the appropriate spin state could pass through the polarizing foil (now serving as an analyzer) and finally these neutrons were diverted to a detector

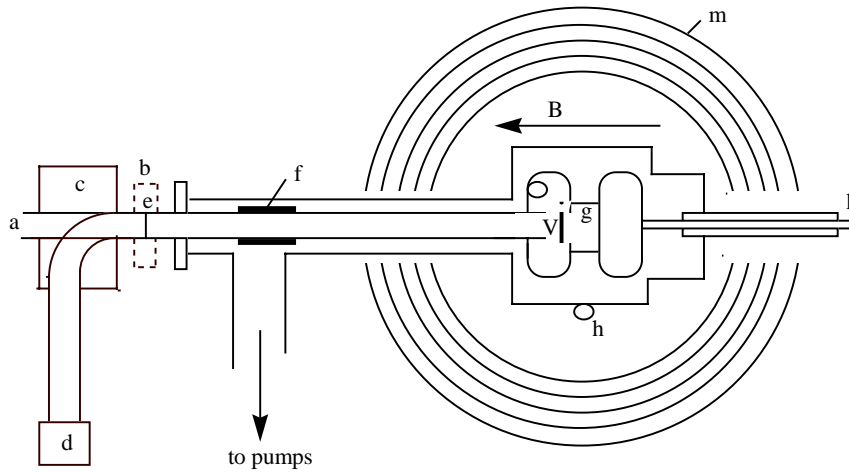


Fig. 4. Schematic diagram of 1990 I.L.L. neutron EDM expt. a:UCN entrance; b: magnet; c: guide changer; d: UCN detector; e: polarizing foil; f: flip coil; g: storage chamber; v: neutron valve; k: rubidium magnetometer; m: 5 layer magnetic shield; p: HV feedthrough.

and counted. The result of this experiment is:

$$d_n = (-3 \pm 5) \cdot 10^{-26} \text{ e cm} \quad (22)$$

A comparable result was obtained in a somewhat similar experiment at St. Petersburg.<sup>24</sup>

The 1990 I.L.L. experiment was limited in precision by uncertainties in the magnetic field as determined by 3 separated Rb magnetometers. In a new version of the same experiment<sup>25</sup> that is presently collecting data, the magnetic field inside the bottle is monitored by optically pumped  $^{199}\text{Hg}$  vapor that fills the bottle uniformly (see Fig.5). This and a variety of other improvements make it possible that the current I.L.L. experiment will ultimately yield a result at the  $3 \cdot 10^{-26}$  e cm level of precision. (Note, however, that the neutrons are so cold that *they* do not fill the bottle uniformly, but sink gradually toward the bottom! Hence, even in this experiment the magnetometer and the neutrons are not exactly in the same place). New and different experimental methods are needed if  $d_n$  is to be measured to much better precision. Following ideas originally presented by Golub and Pendlebury,<sup>26</sup> Golub and Lamoreaux<sup>27</sup> have suggested the following scheme, now in development at Los Alamos National Laboratory. UC

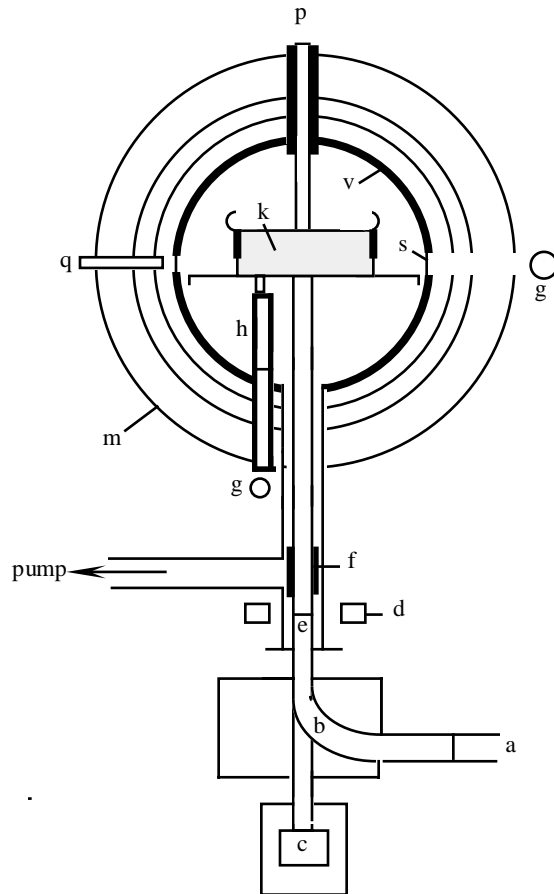


Fig. 5. Schematic diagram of the current I.L.L. neutron EDM experiment. a: UCN source; b: neutron guide change-over; c: UCN detector; d: magnet; e: polarizing foil; f: flip coil; g: Hg UV lamps; h: cell for pre-polarization of Hg atoms; k: storage volume; m: 4-layer magnetic shield; p: HV lead; q: UV light detector; v: vacuum wall; s: optical windows.

neutrons are to be trapped in a storage vessel containing superfluid  $^4\text{He}$  plus a dilute solution of polarized  $^3\text{He}$ . Neutrons at rest or nearly so in superfluid  $^4\text{He}$  can only absorb a  $^4\text{He}$  excitation, the energy  $E^*$  and momentum of which lie at the intersection of the  $^4\text{He}$  phonon-roton dispersion curve and the free neutron dispersion curve (see Fig. 6). However,  $E^* \gg kT$ ; hence the Boltzmann factor  $\exp(-E^*/kT)$  is much less than unity and the loss rate of UC neutrons by scattering on  $^4\text{He}$  is very small. Therefore it is possible to build up a number density of UC neutrons orders-of-magnitude greater than in previous experiments. The role of  $^3\text{He}$  is as follows. The cross section for absorption of neutrons by the reaction  $^3\text{He}(n,p)^3\text{H} + 764 \text{ keV}$  is very large, but only in the  $J=0$  spin state of  $n$  and  $^3\text{He}$ , (where the spins of these two species are opposed). Thus, observation of this spin-dependent reaction by means of the resulting scintillations in  $^4\text{He}$  provides a means for detecting the precession of the neutron EDM in an applied electric field. As in previous and present neutron EDM experiments, it is critically important to monitor the magnetic field precisely. In principle, this can be done by using the  $^3\text{He}$  as a magnetometer. This proposed experiment has many interesting and subtle technical problems, and may take quite a few years to complete.

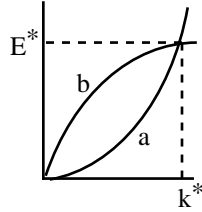


Fig. 6. Sketch of dispersion curves for a) free neutron; b) superfluid  $^4\text{He}$ .

## 6 General remarks about atomic and molecular EDMs

It is obviously impractical to observe the EDM of an electron or bare nucleus by placing it in an external  $E$  field, since that particle would quickly be accelerated out of the region of observation. Thus one is led to ask what can be done with a neutral atom or molecule that contains a nucleus or an electron with an EDM  $d$ . At first sight, this appears to be an unprofitable approach, because in the point-charge, non-relativistic limit, the atom itself would not possess an EDM  $d_a$  (would not exhibit a linear Stark effect), even if

d were non-zero. For, neither the atom nor any of its constituents is accelerated in an external electric field  $\mathbf{E}$ , and in the non-relativistic point-charge limit, where all atomic forces are electrostatic, the *average* electric field at the nucleus or at any electron must be zero. (The electronic and nuclear charges rearrange themselves to cancel the external electric field). This argument is easily cast in quantum-mechanical form and is known as "Schiff's theorem".<sup>28</sup> However, as was first pointed out by Schiff, the theorem does not hold for the nucleus when one takes into account magnetic hyperfine structure, or finite nuclear size if in the latter case the nuclear electric dipole distribution and the nuclear charge distribution are not the same. In this case the nucleus may possess a "Schiff moment"  $Q$ , which has dimensions  $e \text{ cm}^3$  and results in non-zero  $d_a$ .

Sandars<sup>29</sup> showed that Schiff's theorem also fails for an unpaired atomic electron in a paramagnetic atom, when relativistic effects are taken into account (here we recall the all-important factor  $\gamma^0$  in the first term on the right hand side of(21)). Sandars demonstrated that in paramagnetic atoms such as the alkalis and thallium, the ratio  $R=d_a/d_e$  is of order  $10 Z^3 \alpha^2$  where  $Z$  is the atomic number and  $\alpha$  is the fine structure constant. Thus the "enhancement factor"  $R$  can be much larger than unity, and in fact one calculates  $R=115$  for Cs ( $Z=55$ ) and  $R=-585$  for Tl ( $Z=81$ ); (see Table 4). Enhancement factors for certain paramagnetic polar molecules (e.g. YbF, PbO, ...) are orders-of-magnitude larger. Sandars' important discovery provides the basis for all modern electron EDM searches - one attempts to observe the linear Stark effect of the appropriate neutral paramagnetic atom or molecule in an external field, and interprets the result in terms of  $d_e$  by means of a calculated enhancement factor  $R$ .

Table 4. Calculated enhancement factors  $R$

Atom	Z	State	R
Na	11	$3^2S_{1/2}$	0.3
Rb	37	$5^2S_{1/2}$	30
Cs	55	$6^2S_{1/2}$	115
Fr	87	$7^2S_{1/2}$	1100
<b>Tl</b>	<b>81</b>	<b><math>6^2P_{1/2}</math></b>	<b>-585</b>

However, it is important to note that an atomic or molecular EDM could arise from other contributions besides a nucleon EDM and/or an electron EDM. P,T-odd nucleon-nucleon (N-N) interactions might generate a nuclear EDM and thus a Schiff moment.<sup>30</sup>

P,T odd electron-nucleon (e-N) interactions might also exist.<sup>31</sup> These as well as the P,T-odd NN interactions could appear in one or several non-derivative coupling forms: "scalar", "tensor", and "pseudoscalar" (although the last of these is only capable of making a very small contribution). Finally, as was noted earlier, C,T odd (P even) e-N and N-N interactions and possible T-odd beta decay couplings could cause an EDM through radiative corrections involving the standard-model weak interactions.<sup>6,9</sup> So far, experiments on the diamagnetic atom  $^{199}\text{Hg}$  (see below) provide the best limits on P,T-odd N-N interactions and the tensor form of the P,T-odd eN interaction. Meanwhile an experiment on the paramagnetic atom  $^{205}\text{Tl}$  (see below) provides the best limit on  $d_e$  and the scalar form of the P,T-odd eN interaction.

## 7 Diamagnetic atoms

A precise experiment on  $^{199}\text{Hg}$  has been carried out by E.N. Fortson and co-workers at U. Washington, Seattle.<sup>32</sup> (See Fig.7.)  $^{199}\text{Hg}$  was chosen for the following reasons: first,  $Z=80$  is large, and the nuclear-spin-dependent effects that contribute to the Schiff moment scale roughly as  $Z^2$ . Second, the ground electronic state of Hg is  $^1S_0$ , (there is no net electronic angular momentum), and the nuclear spin of  $^{199}\text{Hg}$  is  $I=1/2$ . Hence nuclear-spin-polarized  $^{199}\text{Hg}$  vapor in a cell has a very long spin relaxation time, because the usual electric quadrupole relaxation mechanisms are absent here. Large polarization in a dense sample ( $n \approx 10^{13} \text{ cm}^{-3}$ ) is thus quite easily produced by optical pumping with the 254 nm resonance line, and precession induced by an EDM in an external electric field would readily be monitored by the same optical pumping. The main systematic uncertainties arise from possible stray magnetic fields from charging and leakage currents that reverse with electric field. The result is:

$$d(^{199}\text{Hg}) = (-1.0 \pm 2.4 \pm 3.6) \cdot 10^{-28} \text{ e cm}. \quad (23)$$

where the first uncertainty is statistical and the second is systematic. Combining these one finds the upper limit:

$$d(^{199}\text{Hg}) \leq 8.7 \cdot 10^{-28} \text{ e cm}. \quad (95\% \text{ confidence}) \quad (24)$$

This is the most precise of all experimental EDM limits. Its implications for various P,T-odd effects are summarized in Table 5. Fortson and co-workers have now embarked on a new version of the experiment, by which they hope to improve the precision by

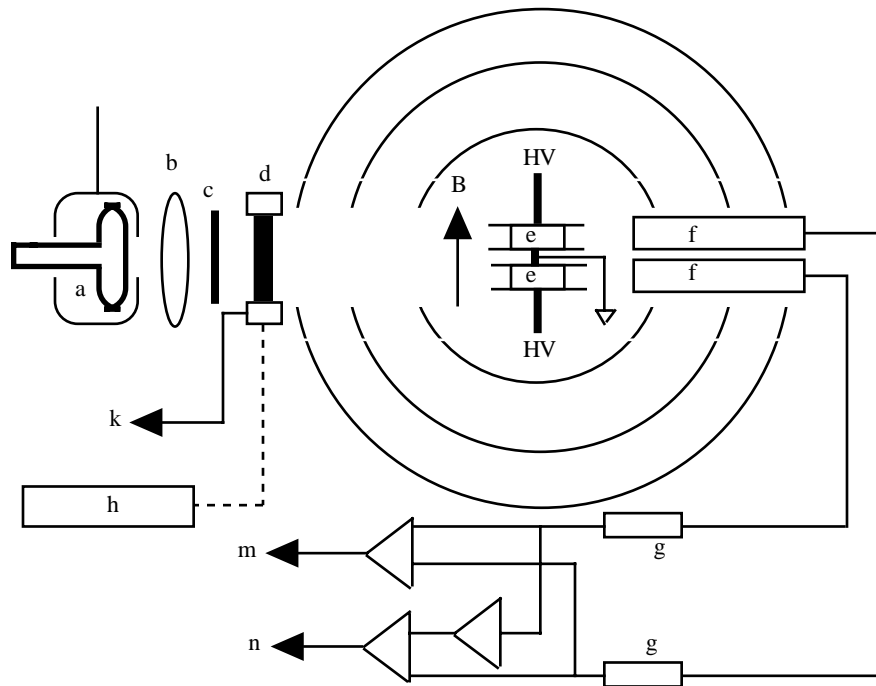


Fig. 7. Schematic diagram of Seattle  $^{199}\text{Hg}$  EDM experiment. a:  $^{204}\text{Hg}$  lamp; b: lens; c: linear polarizer; d: quarter-wave plate; e: optical pumping cells; f: optical detectors; g: phase sensitive detectors; h: stepping motor; k: phase sensitive detector reference; m: magnetic field and gradient correction signals.

an order of magnitude. This gain might be realized by several major improvements, including replacement of the 254 nm light source (formerly a discharge lamp) by a laser; increase in the mercury vapor density, and use of 4 stacked mercury vapor cells to detect and subtract spurious magnetic fields, rather than the two cells previously used.

R. Walsworth of Harvard-Smithsonian, T. Chupp of Michigan, and co-workers<sup>33</sup> have constructed a  $^{129}\text{Xe}$ ,  $^3\text{He}$  2-species noble gas maser that may permit a precise EDM experiment on  $^{129}\text{Xe}$  analogous to that on  $^{199}\text{Hg}$ ; (see Fig. 8). The apparatus consists of two connected cells containing  $^{129}\text{Xe}$ ,  $^3\text{He}$ , rubidium vapor, and  $\text{N}_2$  buffer gas. Polarization of  $^{129}\text{Xe}$  and  $^3\text{He}$  is produced by spin exchange with optically pumped Rb vapor in the pump bulb. The spin-polarized xenon and helium diffuse into the maser bulb, where maser oscillations occur at audio frequencies on the nuclear spin-1/2

Zeeman transitions in a static magnetic field. The two-chamber configuration permits excellent frequency stability. The  $^3\text{He}$  functions as a "co-magnetometer" to monitor the magnetic field, and thus guard against systematic errors arising from leakage and charging currents that might change with the sign of the electric field.

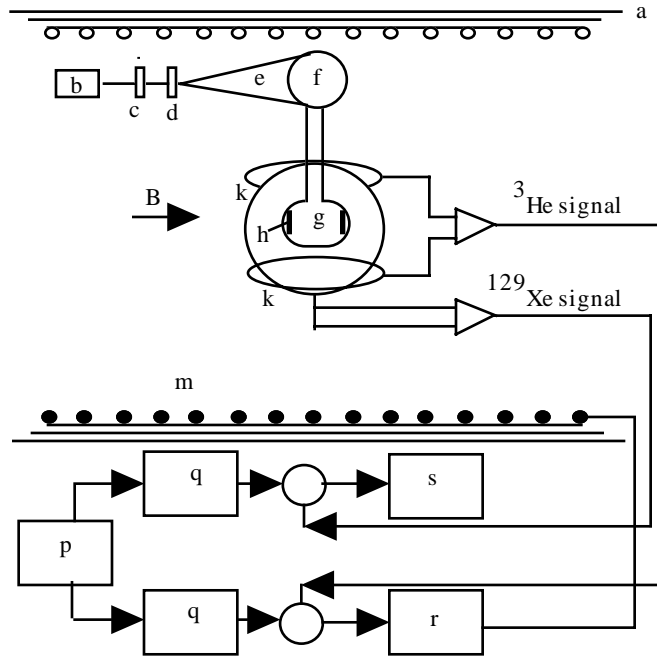


Fig. 8. Schematic diagram of Harvard/Smithsonian-Michigan  $^{129}\text{Xe}$  EDM experiment. a: nested magnetic shields; b: 795 nm light source; c: quarter wave plate; d: beam expander; e: light beam; f: pump bulb; ( $T=120\text{ C}$ ); g: maser bulb; ( $T=40\text{ C}$ ); h: electric field plates; h: pickup coils; m: main solenoid; p: LORAN reference; q: frequency synthesizers; r: phase-sensitive current source; s: A/D converter.

## 8 Paramagnetic atoms

In 1989, L. Hunter and co-workers<sup>34</sup> performed an optical pumping experiment on cesium, and obtained the result:

$$d(\text{Cs}) = (-1.8 \pm 6.7 \pm 1.8) \cdot 10^{-24} \text{ e cm} \quad (25)$$

which implies

$$|d_e| \leq 9 \cdot 10^{-26} e cm \quad (26)$$

More recently, electron EDM experiments on Cs have been suggested that would utilize the methods of atom trapping and cooling.<sup>35</sup> Heinzen and co-workers<sup>36</sup> have analyzed the limitations imposed by collisions on the precision that can be achieved by such an experiment. The trapping of cesium atoms in cold solid <sup>4</sup>He has been studied experimentally, and it may offer interesting possibilities for an EDM search.<sup>37</sup>

At present, however, the best limit on  $d_e$  is derived from the Berkeley experiment<sup>38</sup> on <sup>205</sup>Tl. Here the atomic beam magnetic resonance method with separated oscillating fields was employed, (see Fig.9). The experiment was performed in a weak uniform magnetic field that defined the axis of quantization  $z$ ; (typically  $B_z = 0.4$  Gauss). A strong electric field  $\mathbf{E}$  (typically 107 kV/cm) was placed between two oscillating rf field regions and was nominally parallel to  $\mathbf{B}$ . In order to minimize an important possible systematic effect ( the " $\mathbf{E} \times \mathbf{v}$ " effect arising from precession of the atomic magnetic moment in the motional magnetic field) two counterpropagating beams of atomic Tl were utilized, travelling in the vertical direction to minimize the effects of gravity. The final result was:

$$d(^{205}Tl) = (-1.05 \pm .70 \pm .59) \cdot 10^{-24} e cm \quad (27)$$

Assuming an enhancement factor  $R = -585$  and ignoring all possible contributions to  $d(^{205}Tl)$  except for  $d_e$ , one obtains from (27) the result:

$$d_e = (1.8 \pm 1.2 \pm 1.0) \cdot 10^{-27} e cm \quad (28)$$

Some further implications of this result are summarized in Table 5. Analysis of the main sources of noise and systematic uncertainty in this experiment led us to conclude that the overall uncertainty could be reduced by an order-of-magnitude through several basic improvements that have now been implemented (see Fig. 10). The new experiment functions according to the same general plan as the previous one, but utilizes two up-beams issuing from a common oven with two source slits, as well as two down-beams. These beams are separated by 2.5 cm and pass through separate state selectors, collimating slits, rf regions, and analyzer-detector regions, but *opposite* electric fields. However the magnetic field is essentially the same for each beam. Thus the EDM asymmetry is of opposite sign for the two beams, but many sources of noise are highly correlated ("common mode") for the two beams. Thus when the difference in the signal asymmetries of the two beams is measured, the noise is sharply reduced. In another

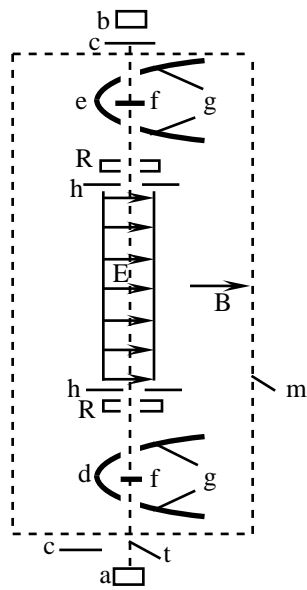


Fig. 9. Schematic diagram of 1994 Berkeley  $^{205}\text{Tl}$  electron EDM experiment. a: up-beam oven; b: down-beam oven; c: automatic beam stops; d: state selector region; e: analyzer region; f: 378 nm laser beams ( $\perp$  to page); g: 535 nm fluorescence; h: collimating slits; E: 107 kV/cm electric field; B: static magnetic field; m: 4-layer magnetic shield; R: radio frequency field regions; t: Tl atomic beam.

basic improvement, each up-beam and each down-beam actually consists of atomic sodium as well as atomic thallium issuing simultaneously from each source. Since the atomic number of sodium is  $Z=11$ , the enhancement factor is only  $R(\text{Na}) = 0.3$ . Thus sodium cannot exhibit an observable EDM effect, but is even more sensitive to various systematic effects than is thallium; hence sodium is an effective "comagnetometer". At present this experiment has achieved a statistical precision of  $3 \cdot 10^{-28}$  e cm in  $d_e$ , but a subtle systematic effect has so far prevented us from achieving a final result. We hope to overcome this problem in the near future.

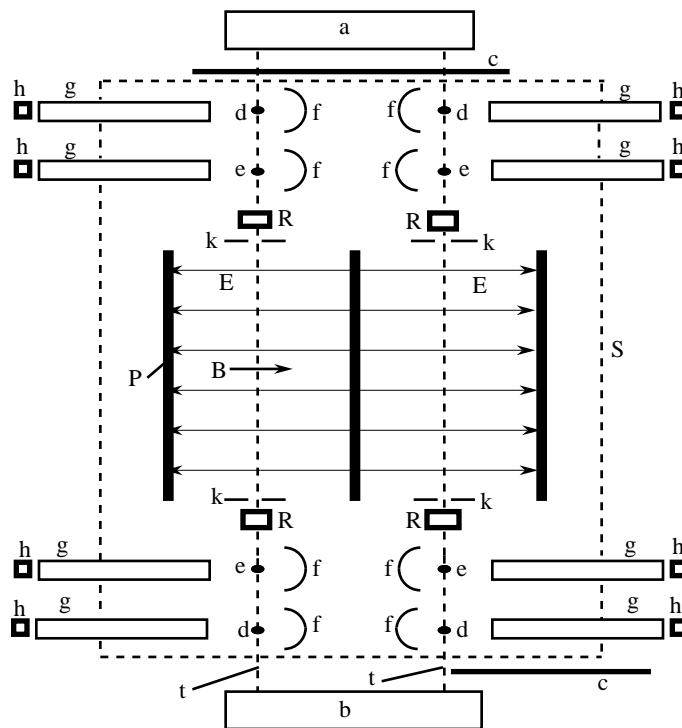


Fig. 10. Schematic diagram of present Berkeley electron EDM experiment. a:down beam oven; b: up beam oven; c: automatic beam stops; d: 378 nm laser beams for Tl ( $\perp$  to page); e: 589 nm laser beams for Na ( $\perp$  to page); f: aluminum reflectors; g: light pipes; h: photodiode detectors; k:collimating slits; P: electric field plates (length 1m., gap 2mm.); R: radio-frequency regions; S: 4-layer magnetic shield; B: uniform magnetic field; E: electric field (120 kV/cm.); t: Na-Tl atomic beams.

## 9 Paramagnetic molecules

Certain paramagnetic polar diatomic molecules are very attractive candidates for experimental electron EDM searches, because their enhancement factors are orders-of-magnitude larger than that of atomic thallium.<sup>39</sup> The list of proposed molecules includes BaF, CdF, YbF, HgF, PbF, PbO, and several others as well. They have large enhancements because the spin-rotational levels of opposite parity that are mixed by P,T-odd EDM interactions lie much closer together (by factors of  $\approx 10^3$ ) than do the analogous levels of paramagnetic atoms. Kozlov and Labzowsky<sup>40</sup> have reviewed calculations of the enhancement factors by a variety of semi-empirical and ab-initio methods.

Consider a typical heavy metal-fluorine molecule MF. Typically M in its normal state has two 6s valence electrons, while the ground configuration of the F atom is  $1s^2 \dots 2p^5$ . In the MF molecule, one of the 6s electrons is transferred to the fluorine, thereby completing its p shell and creating an ionic bond with a corresponding molecular electric dipole moment that is typically 3-5 Debye units. The remaining 6s electron moves in a highly polarized orbit in the strong molecular electric field directed along the internuclear axis between  $M^+$  and  $F^-$ . This unpaired electron is the analog of the valence electron in atomic thallium or cesium. If one applies an external E field that is sufficiently strong to generate Stark shifts comparable to the spin-rotational splittings, the internuclear axis becomes aligned with the external E field. For the molecules we have mentioned, this can be achieved with practical laboratory E fields.<sup>41,42</sup> However, the molecular experiments are difficult for diverse reasons, and new results are likely to be slow in coming. One final remark concerning molecules: An experiment<sup>43</sup> on the diamagnetic molecule TlF provides us with the best limit on the EDM of the proton, (see Table 5). However this limit is much less significant than the limit on the neutron EDM.

## 10 The Muon EDM

Until now, the only way to search for the muon EDM  $d_\mu$  is to observe the precession of free relativistic muons in a magnetic field. In an important experiment carried out at the CERN muon storage ring more than 20 years ago,<sup>44</sup> the limit:

$$d_{mu} \leq 7 \cdot 10^{-19} \text{ e cm} \quad (29)$$

Table 5. Summary of EDM results from neutron, atomic, and molecular expts.

P,T viol. param.	System	Upper limit	Ref.
$d_n$	n	$8 \cdot 10^{-26}$ e cm	23
QCD phase $\Theta_{QCD}$	n	$4 \cdot 10^{-10}$	23
$d_{Diamag.mol}(TIF)$	TIF	$4.6 \cdot 10^{-23}$ e cm	43
$d_{proton}$	TIF	$1 \cdot 10^{-23}$ e cm	43
Schiff moment $Q_S(^{205}Tl)$	TIF	$1 \cdot 10^{-9}$ e cm	43
$d_a(^{199}Hg)$	$^{199}Hg$	$8.7 \cdot 10^{-28}$ e cm	32
Schiff moment $Q_S^{199}Hg)$	$^{199}Hg$	$2.2 \cdot 10^{-11}$ e cm	32
$\eta^{(a)}$	$^{199}Hg$	$1.6 \cdot 10^{-3}$	32
$\eta_q^{(b)}$	$^{199}Hg$	$3.4 \cdot 10^{-6}$	32
$C_T^{(c)}$	$^{199}Hg$	$1.3 \cdot 10^{-8}$	32
Supersym. $\epsilon_q^{SUSY}$	$^{199}Hg$	$7 \cdot 10^{-3}$	32
$d_e$	$^{205}Tl$	$4 \cdot 10^{-27}$ e cm	38
$C_S^{(d)}$	$^{205}Tl$	$4 \cdot 10^{-7}$	38
Supersym. $\epsilon_e^{SUSY}$	$^{205}Tl$	$4 \cdot 10^{-2}$	38

- a) Coupling constant in scalar P,T-odd NN interaction.
- b) Coupling constant in scalar P,T-odd quark-quark interaction.
- c) Coupling constant in tensor P,T-odd e-N interaction.
- d) Coupling constant in scalar P,T-odd e-N interaction.

was established simultaneously with a measurement of the muon g-factor anomaly  $a = (g-2)/2$ . Muons from pion decay with an initial polarization  $P \geq 95\%$  travelled around the 14 m. dia storage ring in a horizontal plane. A homogeneous vertical magnetic field was applied, and weak vertical focussing was provided by an electrostatic quadrupole field. The precession of the muon spin in these circumstances is described by the famous Bargmann-Michel-Telegdi equation.<sup>45</sup> An EDM causes the precession to be modified slightly because in the muon's rest frame there exists not only a magnetic field, but also a motional electric field to which the EDM is coupled, (See Fig. 11).

A dedicated experiment of the same type has been proposed with the much larger muon storage ring at Brookhaven National Laboratory (which has already been used to improve substantially the precision in determination of g-2). It appears possible in principle to improve the limit on the muon EDM by approximately 4 orders of magnitude.<sup>46</sup>

## 11 Weak dipole moment and EDM of the tau lepton

Finally we mention the tau lepton, which must of course be investigated by the methods of high-energy physics. Taus are produced in  $e^+e^-$  collisions at colliding beam accelerators:

$$e^+e^- \rightarrow \tau^+\tau^- \rightarrow (A^+\nu) + (B^-\bar{\nu}) \quad (30)$$

The tau production reaction occurs in lowest order by two amplitudes: photon exchange (electromagnetic interaction) and  $Z^0$  exchange (neutral weak interaction). When the  $e^+e^-$  CM energy is in the vicinity of the Z resonance at 91 GeV, as in various experiments at LEP, the Z amplitude greatly dominates. The mean life of the tau is only  $2.9 \cdot 10^{-13}$ s., and it decays in a variety of modes represented schematically in (30) by  $A^+\nu$  and  $B^-\bar{\nu}$ . In principle, CP violation could occur at the  $eeZ$  vertex, at the  $Z\tau\tau$  vertex, and/or in the decays of  $\tau^+$  and  $\tau^-$ . However, if  $e^+$  and  $e^-$  are unpolarized it can be shown that there are no observable CP violating effects at the  $eeZ$  vertex. Furthermore, it seems likely that new CP violation effects would be associated with the vertex at which there is the largest momentum transfer; hence one concentrates on the  $Z\tau\tau$  vertex. In order to describe CP violation one then writes the following Lagrangian density:

$$\mathcal{L}_{EDM} = -\frac{i}{2}\bar{\Psi}\gamma^5\sigma^{\mu\nu}\Psi[d_\tau F_{\mu\nu} + \bar{d}_\tau(\partial_\mu Z_\nu - \partial_\nu Z_\mu)] \quad (31)$$

Here,  $\Psi$  is the Dirac field describing the tau,  $Z_\nu$  is the Z-boson vector potential, and  $d_\tau, \bar{d}_\tau$  are the EDM and the "weak dipole moment" (WDM) of the tau, respectively. Strictly speaking the latter quantities depend on the square of the 4-momentum transfer  $q^2$ ;  $d_\tau(q^2 = 0)$  is by definition the EDM, while  $\bar{d}_\tau(q^2 = m_Z^2)$  is defined as the WDM. While there is no explicit relationship between  $d_\tau$  and  $\bar{d}_\tau$  they are expected to be roughly the same in most models of CP violation. Near the Z resonance only  $\bar{d}_\tau$  term in the Lagrangian density is important.

The transition amplitude  $T$  for reaction (30) to a specific final state can be written quite generally as:

$$T = T_{SM} + T_{CP} \quad (32)$$

where  $T_{SM}$  is the CP-conserving (standard model) part, while  $T_{CP}$  is the CP violating part. Then the differential cross-section is proportional to:

$$|T_{SM} + T_{CP}|^2 = (|T_{SM}|^2 + |T_{CP}|^2) + (T_{SM}T_{CP}^* + cc) \quad (33)$$

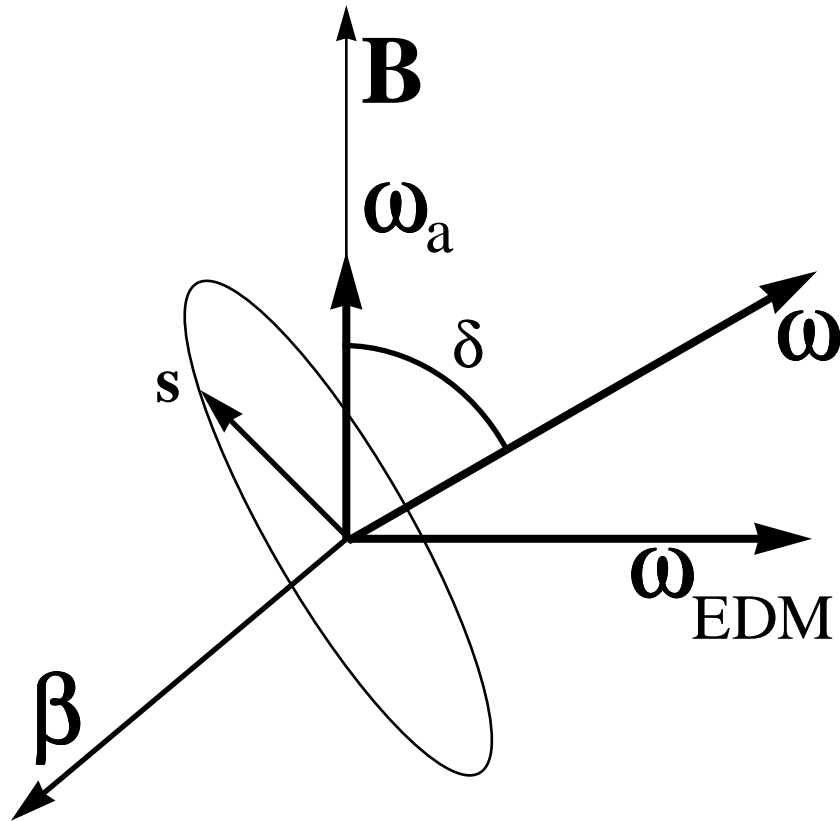


Fig. 11. Schematic diagram (not to scale) of relevant vectors in muon spin-precession experiment, as described by the BMT equation.  $\beta$ : muon velocity;  $\mathbf{B}$ : applied magnetic field;  $\omega_a$ : ang. vel. of precession due to  $g-2$ ;  $\omega_{EDM}$ : ang vel of precession due to EDM;  $\omega$ : resultant;  $\delta$ : angle between  $\omega$  and  $\mathbf{B}$ ;  $\mathbf{s}$ : muon spin vector, which precesses about  $\omega$ .

The first quantity in parentheses on the right hand side of (33) is CP-even and is proportional to the total cross-section, or in other words, to the partial width  $\Gamma_{\tau\tau}$  for Z decay to  $\tau\tau$ . The second ("interference") term in parentheses on the right hand side of (33) manifests itself in certain CP-odd observables (correlations) in the differential cross-section.<sup>47</sup> These correlations are related to the spins of the outgoing tau leptons, but the latter are not directly observable. Instead, because of their short lifetime, the taus decay very close to their point of origin, and information about their spins is transferred to the energies and momenta of the decay products  $A^+B^-$ . The latter quantities must be observed to determine  $\overline{d_\tau}$ .

Two experiments have been carried out at LEP. One employed the OPAL detector; the other was performed at the ALEPH detector.<sup>48</sup> Combining these results one obtains the limit:

$$\overline{d_\tau} \leq 5.8 \cdot 10^{-18} \text{ e cm} \quad (34)$$

More precise limits might be obtained in the future by means of experiments at the proposed "Tau-charm factory". Here it might be possible to employ longitudinally polarized electrons, and thus use more convenient P,T-odd correlations.

## References

- [1] E. G. Adelberger and W.C. Haxton, *Annu. Rev. Nucl. Part. Sci.* **35**, 501 (1985).
- [2] L. Dobrzynski et. al., *Phys. Lett.* **22**, 105 (1966).
- [3] E. Blanke et. al., *Phys. Rev. Lett.* **51**, 355 (1983).
- [4] D. Boose, H. L. Harney, and H. A. Wiedenmuller, *Phys. Rev. Lett.* **56**, 2012 (1986); *Z. Phys. A* **325**, 363 (1986); J.B. French, V.K. Kota, A. Pandey, and S. Tomsovic, *Phys. Rev. Lett.* **54**, 2313 (1985); *Ann. Phys. (N.Y.)* **181**, 198 (1988).
- [5] J. E. Koster et. al., *Phys. Lett. B* **267**, 23 (1991).
- [6] M. J. Ramsey-Musolf, *Phys. Rev. Lett.* **83**, 3997 (1999).

- [7] J. D. Jackson, S. B. Treiman, and H.W. Wyld, Nucl. Phys. **4**, 206 (1957).
- [8] C. G. Callan and S. B. Treiman, Phys. Rev. **162**, 1494 (1967).
- [9] I. B. Khriplovich, JETP Lett. **52**, 461 (1990).
- [10] R. I. Steinberg et. al., Phys. Rev. Lett. **33**, 41 (1974).
- [11] A. V. Vorobiov et. al., Nucl. Instr. Methods A **284**, 127 (1989).
- [12] S. Freedman, private communication (1999).
- [13] A. L. Hallin et. al. Phys. Rev. Lett. **52**, 337 (1984).
- [14] M. Abe et. al. (KEK-E246 Collaboration), Phys. Rev. Lett. **83**, 4253 (1999).
- [15] L. Landau, Sov. Phys. JETP **5**, 336 (1957).
- [16] W. G. Penney, Phil. Mag. **11**, 602 (1931).
- [17] E. E. Salpeter, Phys. Rev. **112**, 1642 (1958).
- [18] E. P. Shabalin, Sov. J. Nucl. Phys. **28**, 75 (1978); Sov. Phys. Usp. **26**, 297 (1983);  
T. Donoghue, Phys. Rev. D **18**, 1632 (1978).
- [19] X. He, B. H. J. McKellar, and S. Pakvasa, Int. J. Mod. Phys. A **4**, 5011 (1991); A.  
Czarnecki and B. Krause, Phys. Rev. Lett. **78**, 4339 (1997).
- [20] F. Hoogeveen, Nucl. Phys. B **341**, 322 (1990).
- [21] M. Pospelov and I. B. Khriplovich, Sov. J. Nucl. Phys. **53**, 638 (1991).

- [22] N. F. Ramsey, Phys. Rev. **76**, 996 (1949); *Molecular Beams* (Oxford University Press, Oxford, 1990), p.365.
- [23] K. F. Smith, et. al., Phys. Lett. B **234**, 191 (1990).
- [24] I. S. Altarev et. al., Phys. Atomic Nucl. **54**, 1152 (1996).
- [25] P. G. Harris et. al., Phys. Rev. Lett. **82**, 904 (1999).
- [26] R. Golub, and J. M. Pendlebury, Phys.Lett. A **53**, 133 (1975); Rep. Prog. Phys. **42**, 439 (1979).
- [27] R. Golub and S. K. Lamoreaux, Phys. Rep. **237**, 1 (1994).
- [28] L. I. Schiff, Phys. Rev. **132**, 2194 (1963).
- [29] P. G. H. Sandars, Phys. Lett. **14**, 194 (1965); Phys. Lett.**22**, 290 (1966).
- [30] O. P. Sushkov, V. V. Flambaum, and I. B. Khriplovich, Sov. Phys. JETP **60**, 873 (1984); V. V. Flambaum,I. B. Khriplovich, O. P. and Sushkov, Phys. Lett. B **162**, (1985); Nucl. Phys. A **449**, 750 (1986); V. M. Khatsymovsky,I. B. Khriplovich, and A. S. Yelkhovsky, Ann. Phys. **186**, 1 (1988); W. C. Haxton, and E. M. Henley, Phys. Rev. Lett. **51**, 1937 (1983); X. He and B. McKellar, Phys. Lett. B **62**, 97 (1976); I. B. Khriplovich, Sov. Phys. JETP **4**, 25 (1976); V. F. Dmitriev, I.B. Khriplovich, and V. B. Telitzin, Phys. Rev. C **50**,2358 (1994).
- [31] C. Bouchiat, Phys. Lett. B **57**, 284 (1975); E. Hinds, C. Loving, and P. G. H. Sandars, Phys. Lett. B**62**, 97 (1976); V. A. Dzuba, V. V. Flambaum, and V. V. Sylvestrov, Phys. Lett. B **154**, 93 (1985); A. M. Martensson-Pendrill, Phys. Rev. Lett. **54**, 1153 (1985); S. M. Barr, Phys. Rev. Lett. **68**, 1822 (1992); Phys. Rev. D**45**, 4148 (1992);I. B. Khriplovich, Nucl. Phys. B **352**, 385 (1991).

- [32] J. P. Jacobs, W. M. Klipstein, S. K. Lamoreaux, B. R. Heckel, and E. N. Fortson, *Phys. Rev. A* **52**, 3521 (1995).
- [33] R. E. Stoner et. al. *Phys. Rev. Lett.* **77**, 3971 (1996).
- [34] S. A. Murthy, D. Krause, Z. L. Li, and L. Hunter, *Phys. Rev. Lett.* **63**, 965 (1989).
- [35] S. Chu, private communication (1997); D. Weiss, private communication (1999).
- [36] M. Bijlsma, J. Verhaar, and D. Heinzen, *Phys. Rev. A* **49**, R4285 (1994).
- [37] S. I. Kanorsky, S. Lang, S. Lucke, S. B. Ross, T. W. Hansch, and A. Weis, *Phys. Rev. A* **54**, R1010 (1996).
- [38] E. D. Commins, S. B. Ross, D. DeMille, and B. C. Regan, *Phys. Rev. A* **50**, 2960 (1994).
- [39] O. P. Sushkov, and V. V. Flambaum, *Sov. Phys. JETP* **48**, 608 ((1978); V. G. Gorshkov, L. N. Labzowsky, and A. N. Moskalev, *Sov. Phys. JETP* **49**, 414 (1979); V. V. Flambaum, and I. B. Khriplovich, *Phys. Lett. A* **110**, 121 (1985); M. G. Kozlov, *Sov. Phys. JETP* **62**, 1114 (1985); *Sov. J. Quantum Electronics* **18**, 713 (1988); M. G. Kozlov, V. I. Fomichev, Yu. Yu. Dmitriev, L. N. Labzowsky, and A. V. Titov, *J. Phys. B* **20**, 4939 (1988); M. G. Kozlov, and V. F. Ezhov, *Phys. Rev. A* **49**, 4502 (1994).
- [40] M. G. Kozlov and L. N. Labzowsky, *J. Phys. B* **28**, 1933 (1995).
- [41] D. DeMille, Private communication (1997).
- [42] E. Hinds, and B. Sauer, *Phys. World* April, 37 (1997); B. E. Sauer, J. Wang, and E. Hinds, *Phys. Rev. Lett.* **74**, 1554 (1995); *J. Chem Phys.* **105**, 7412 (1996).

- [43] D. Cho, K. Sangster, and E. Hinds, Phys. Rev. A **44**, 278 (1991).
- [44] J. Bailey, et. al. [CERN Muon Storage Ring Collaboration], J.Phys. G **4**, 345 (1978); Nucl. Phys. B **150**, 1 (1979).
- [45] V. Bargmann, L. Michel, and V. L. Telegdi, Phys. Rev. Lett. **2**, 435 (1959).
- [46] Y. Semertzidis, Private communication (1997).
- [47] W. Bernreuther, and O. Nachtmann, Phys. Rev. Lett. **63**, 2787 (1989); W. Bernreuther et. al., Z. Phys. C **43**, 117 (1989); Z. Phys. C **52**, 567 (1991); W. Bernreuther, A. Brandenburg, and P. Overmann, Phys. Lett. B **391**, 413 (1997).
- [48] R. Akers et. al., (OPAL Collaboration), Z. Phys. C **66**, 31 (1995); Buskelic, D. et al., (ALEPH Collaboration), Phys. Lett. B **346**, 371 (1995).